Universität Rostock

Traditio et Innovatio

INSTITUT FÜR PHYSIK

Proton and Helium Injection Into First Order Fermi Acceleration at Shocks:

Hybrid Simulation and Analysis

Adrian Hanusch, Tatyana Liseykina, Mikhail Malkov, Roald Sagdeev

Introduction

Cosmic rays (CR) are most likely accelerated at collisionless shocks in supernova remnants, however, the acceleration mechanism is not entirely understood. One complicated problem is the "injection", a process whereby the shock selects a tiny fraction of particles to keep on crossing its front and gain more energy.

Recent precise measurements of the PAMELA space craft show a difference between He^{2+} and proton spectra [1, 2]. Hence the elemental composition of galactic CR might hold the key to their origin and comparing the injection rates of particles with different mass to charge ratio is a powerful tool for studying the injection process.

We performed a series of one dimensional hybrid simulations and analyzed a joint injection of protons and Helium.

Hybrid Simulation

The dynamics of collisionless shocks can be simulated by means of *hybrid* simulations. In these simulations the ions are treated kinetically,

$$M_i \frac{d\mathbf{v}_i}{dt} = q_i \left(\mathbf{E} + \frac{1}{c} \mathbf{v}_i \times \mathbf{B} - \eta \mathbf{J} \right) \quad \text{and} \quad \frac{d\mathbf{x}_i}{dt} = \mathbf{v}_i, \qquad (1)$$

while the electrons are assumed to be a massless, charge neutralizing fluid,

$$n_e \, m \frac{d\mathbf{v_e}}{dt} = 0 = -e \, n_e \left(\mathbf{E} + \frac{1}{c} \mathbf{v}_e \times \mathbf{B} \right) - \nabla p_e + e \, n_e \, \eta \, \mathbf{J}, \qquad (2)$$

meaning that in this approach the electron scales are neglected. The electron pressure p_e is assumed to be isotropic with an adiabatic relation between pressure and temperature.

$$p_e = n_e \, k_B \, T_e, \qquad \frac{T_e}{T_0} = \left(\frac{n_e}{n_0} \right)^{\gamma - 1}, \qquad (3)$$

where an adiabatic index of $\gamma = 5/3$ is used. In the Maxwell equations the magnetostatic (Darwin) model is employed,

$$\nabla \times \mathbf{B} = \frac{4\pi}{c} \mathbf{J}. \qquad (4)$$

As in usual particle-in-cell simulations, the ion density and current are extrapolated to a grid using a linear weighting,

$$n = \sum_s q_s \int f_s(\mathbf{x}, \mathbf{v}) \, d^3\mathbf{v}, \qquad \mathbf{J_i} = \sum_s q_s \int \mathbf{v} \, f_s(\mathbf{x}, \mathbf{v}) \, d^3\mathbf{v}, \qquad (5)$$

and serve as sources for the calculation of the fields. The electric field,

$$\mathbf{E} = \frac{1}{e\,n} \left(\frac{(\mathbf{J} - \mathbf{J}_i) \times \mathbf{B}}{c} - \nabla p \right) + \eta \, \mathbf{J}, \qquad (6)$$

is calculated via a predictor corrector method and is used for propagating the magnetic field,

$$\frac{\partial \mathbf{B}}{\partial t} = -c \nabla \times \mathbf{E}. \qquad (7)$$

In the simulation dimensionless quantities are used:

t – inverse proton gyrofrequency $1/\omega_c$
x – proton inertial length c/ω_p
v – Alfvén velocity v_A
n – upstream density n_0
B – upstream magnetic field B_0

The ions are initialized in thermal equilibrium with the electrons with a temperature of $T = m v_A^2 / k_B$. Furthermore, a background magnetic field parallel to the shock normal is applied. In order to model the amount of helium in the interstellar matter a fraction of He^{2+} ions of 10% in number density is included.

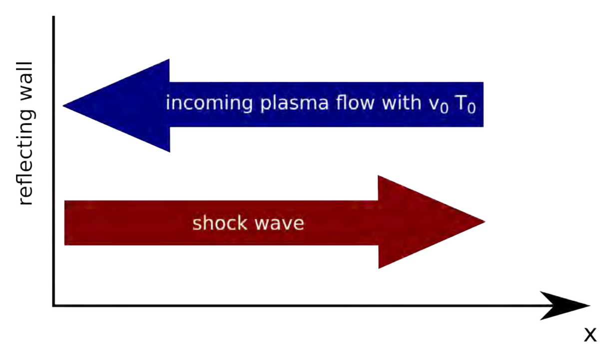

Setup of the simulation: The plasma is flowing with the super sonci velocity v_0 to the right against a reflecting wall. The shock, which forms due to the interaction of the counter steaming beams, is traveling to the right. Hence, the downstream plasma is at rest in the laboratory frame.

All simulations are quasi one-dimensional, which means the spatial dimension is reduced to the propagation direction of the shock but all three components of velocity and fields are included. The size of the simulation box is $L_x = 2000 \, c/\omega_p$ with a grid spacing of $\Delta x = 0.25 \, c/\omega_p$ and 64 particles per cell.

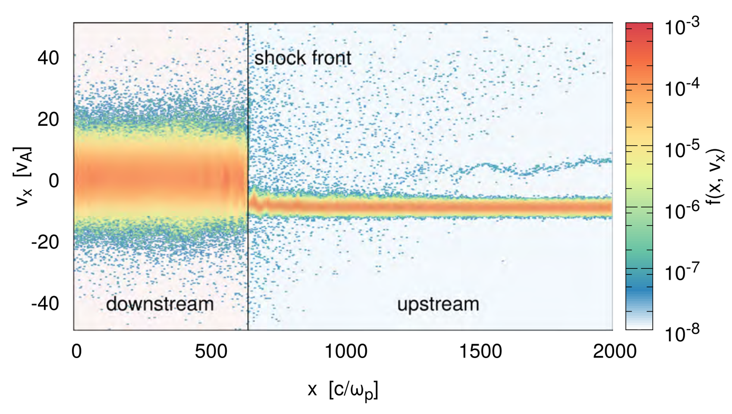

Phase space: after $t = 200 \ 1/\omega_c$ for a simulation without He^{2+} with an initial velocity of $v_0 = 10 v_A$. The shock front is separating the cold upstream and the warm downstream plasma.

Injection efficiency

The injection efficiency is calculated from the velocity distribution of the particles. Maxwellians are fitted to the up- and downstream distributions and the injection efficiency is calculated as

$$\eta_{\mathrm{inj}} = \frac{\int_{v_{\mathrm{inj}}} f_{\mathrm{tot}}(v) - f_{\mathrm{th,up}}(v) - f_{\mathrm{th,down}}(v) \, \mathrm{d}v}{\int f_{\mathrm{tot}}(v) \, \mathrm{d}v}. \qquad (8)$$

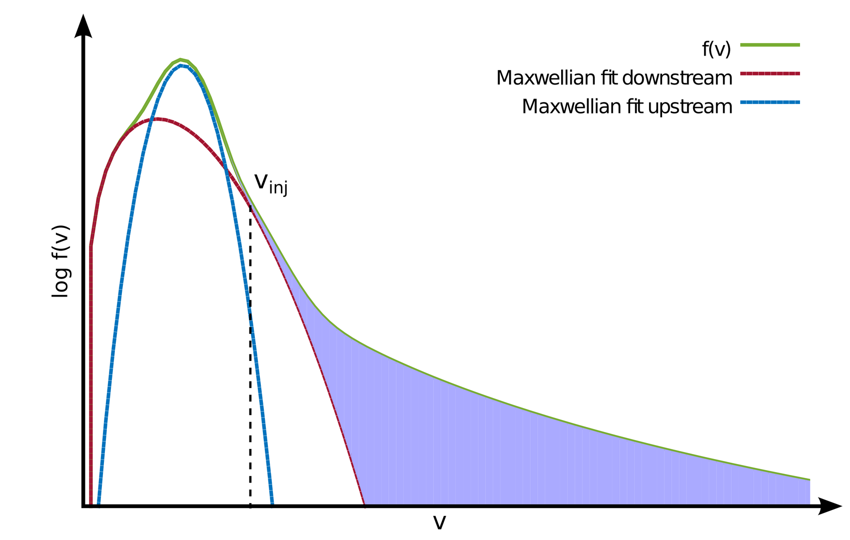

Setup of the simulation: Sketch of the total velocity distribution function $f(v)$ consisting of a shifted Maxwellian distribution upstream, a Maxwellian downstream and a tail containing non-thermal particles.

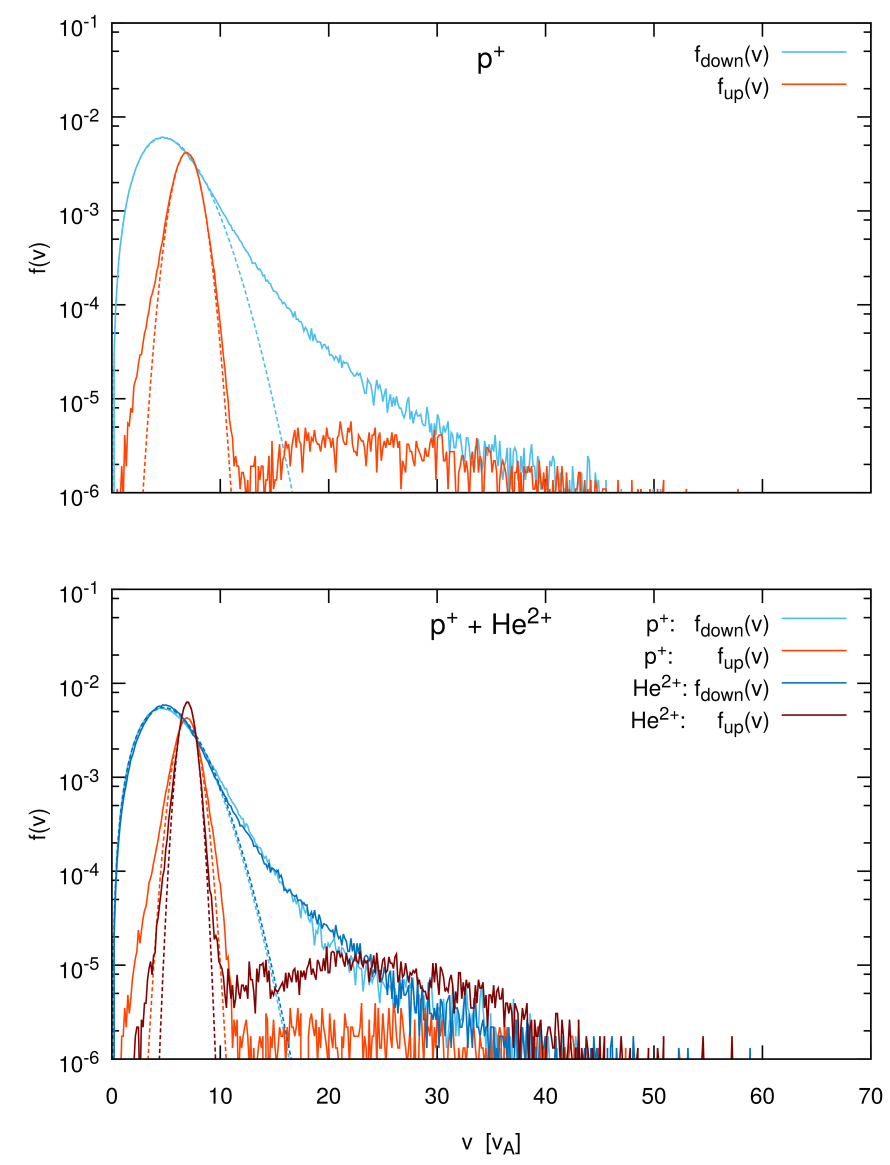

Velocity distribution function: up- and downstream of the shock after $t = 400 \ 1/\omega_c$ for an initial flow velocity of $v_0 = 7$. In the upper panel only protons are present in the simulation, while the lower panel shows results including He^{2+}. Thermal distributions (dashed) are fitted to the up- and downstream distributions.

v_0 $[v_A]$	3.1	5.0	7.0	10.0	15.0
η_{p^+} [%]	0.9	2.9	4.1	5.2	6.1
η_{p^+} [%]	1.4	3.3	4.5	5.8	6.3
$\eta_{\mathrm{He}^{2+}}$ [%]	0.3	1.4	2.6	5.2	6.7

Table 1: Injection efficiency η for different shock velocities for simulations without and with a fraction of He^{2+} ions

During the simulation all particles leaving the simulation box are collected.

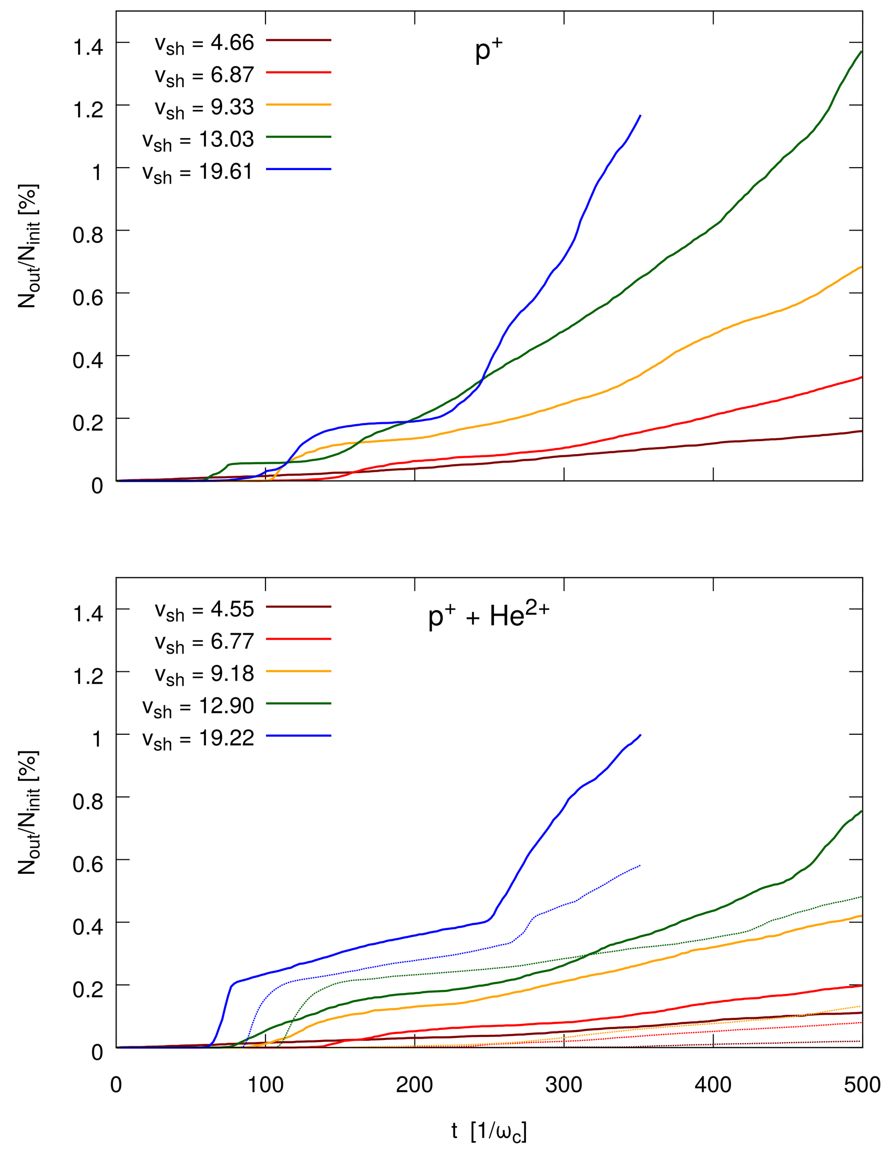

Number of particles leaving the box: Fraction of particles leaving the simulation box over time for different shock velocities. The first sudden increase is caused by particles which are initially reflected at the hard wall.

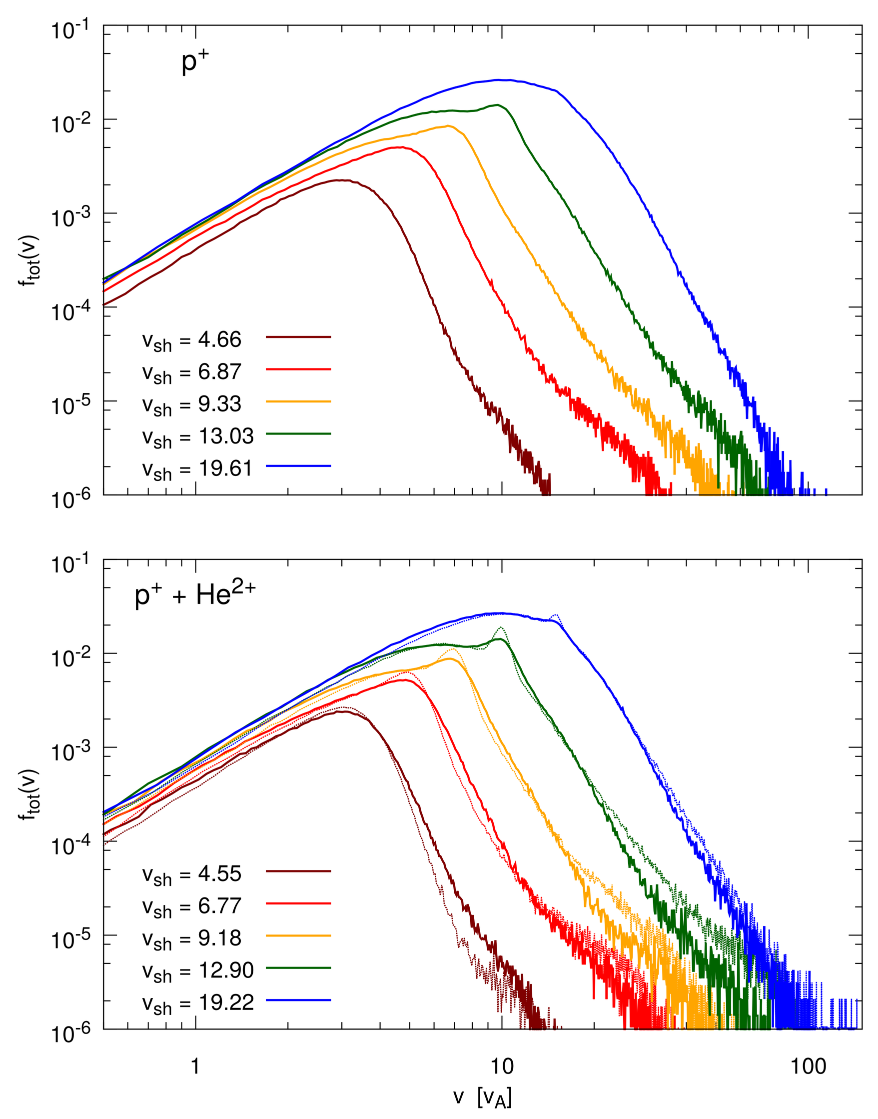

Velocity distribution: at $t = 300 \ 1/\omega_c$ for different v_0. The upper panel shows results for a simulation with protons only, while in the lower plot He^{2+} ions are included. The velocity distribution for the He^{2+} ions (dotted lines) is scaled for better comparison.

Conclusion

•

Outlook

- two- and three-dimensional simulations
- investigation of the upstream waves
- analysis of particle trajectories

References

[1] O. Adriani *et al.*, *Science* 332, 69 (2011).
[2] M. A. Malkov, P. H. Diamond, and R. Z. Sagdeev, *PRL* 108, 081104 (2012).
[3] M. Brics, J. Rapp, D. Bauer. *Phys. Rev. A* 90, 053418 (2014)
[4] B. Feuerstein and U. Thumm. *Journal of Physics B* 36, 707 (2003).
[5] B. Feuerstein and U. Thumm. *Phys. Rev. A* 67, 043405 (2003).